ISBN: 978-3-95450-206-6 doi:10.18429/JACoW-FLS2018-THP2WD01

CONSTRUCTION AND OPTIMIZATION OF CRYOGENIC UNDULATORS AT SOLEIL

M. Valléau* , A. Ghaith, F. Briquez, F. Marteau, P. Berteaud, C. Kitegi, J. Idam, O. Marcouillé, A. Mary, M. Tilmont, J. DaSilva Castro, F. Lepage, K. Tavakoli, J.-M. Dubuisson, N. Béchu, C. Herbeaux, M. Louvet, P. Rommeluére, M. Sebdaoui, A. Lestrade, A. Somogyi, T. Weitkamp, P. Brunelle, L. Nadolski, A. Nadji, M.-E. Couprie,
Synchrotron SOLEIL, GIF-sur-YVETTE , France

Abstract

With permanent magnet undulators operating at cryogenic temperature, the magnetic field and coercivity are enhanced, enabling shorter periods with higher magnetic field. The first full scale (2 m long, 18 mm period) hybrid cryogenic undulator [1] using PrFeB [2] magnets operating at 77 K was installed at SOLEIL in 2011. Photon spectra measurements, in good agreement with the expectations from magnetic measurements, were used for precise alignment and taper optimization. The second and third 18 mm PrFeB cryogenic undulators, modified to a half-pole/magnet/half-pole structure, were optimized without any magnet or pole shimming after assembly, but mechanical sortings and some geometrical corrections had been done before assembly. A systematic error on individual magnets on the third U18 was also compensated. In-situ measurement benches, including a Hall probe and a stretched wire to optimize the undulator field at room and cryogenic temperature are presented. An upgrade of these in-situ benches will be detailed with the fabrication of a 15 mm period and 3 m long PrFeB cryogenic undulator at SOLEIL.

INTRODUCTION

In-Vacuum Undulators (IVU) generate high magnetic field by placing directly the magnets inside the vacuum chamber. Cryogenic Permanent Magnet Undulators (CPMUs) have been developed to reach intense brightness at higher energies as cooling down $RE_2Fe_{14}B$ enables to increase the remanent field and coercivity. The first prototype of 0.6 m length with a period of 14 mm, using high remanence $Nd_2Fe_{14}B$ grade cooled down to 140 K has been developed at SPring-8 [3]. After this first prototype, a 8 x 14.5 mm periods CPMU prototype has been built at Brookhaven National Laboratory (BNL) using $Nd_2Fe_{14}B$ grade reaching a magnetic gap of 5 mm [4–6]. Helmholtz-Zentrum Berlin (HZB) with the collaboration of UCLA, built two CMPU prototypes (20 x 9 mm period and magnetic gap of 2.5 mm), using $Pr_2Fe_{14}B$ magnets cooled down to 20-30 K [7]. At SOLEIL, three hybrid prototypes CPMU have been built and characterized: a 4 periods 18 mm length with $Nd_2Fe_{14}B$ magnets (BH50 Hitachi-Neomax) [8], a 4 x 18 mm period with $Pr_2Fe_{14}B$ (CR53 Hitachi-Neomax) [9], and a 4 x 15 mm period with $Pr_2Fe_{14}B$. The first full-scale cryogenic undulator had been developed at ESRF [10] with a period length of 18 mm using a relatively low remanence $Nd_2Fe_{14}B$ magnet grade (B_r=1.16 T) cooled down to around 150 K, reaching a gap of 6 mm. Then full scale undulators using $Nd_2Fe_{14}B$ based magnets where built for Diamond [11] or at SLS [12]. This article details the design, construction and operation with cryogenic undulators of SOLEIL. U18 n^{o}1 was the first full-scale Praseodymium based magnet undulator installed on a storage ring [2]. The second U18 is in use for COXINEL experiment [13, 14] since 2015 and the third one has been installed in the storage ring since Dec. 2017. A 15 mm period and 3 m long cryogenic undulator (U15) operating at 3 mm gap is also under construction.

MAGNETIC DESIGN

Detailed characterization of $Re_2Fe_{14}B$ permanent magnets have been carried out at SOLEIL [8]. Figures 1 and 2 show the dependence of the remanence and coercivity as a function of the temperature for $Nd_2Fe_{14}B$ and $Pr_2Fe_{14}B$ magnets. When Nd is used, the remanence temperature dependence exhibits a maximum at a temperature between 150 and 100 K, according to the employed grade. It results from the spin transition reorientation (SRT) [15] occurring from this type of magnet. Thus, it requires that Nb based cryogenic undulator to be cooled down to the liquid nitrogen temperature and heated back to the working temperature to 140 K, whereas $Pr_2Fe_{14}B$ based undulators can be directly cooled and operated at 77 K because of the absence of the SRT. Even larger field can be achieved with $Pr_2Fe_{14}B$ magnets by cooling even at lower temperatures than the one of the liquid nitrogen. The cryogenics becomes slightly more complex.

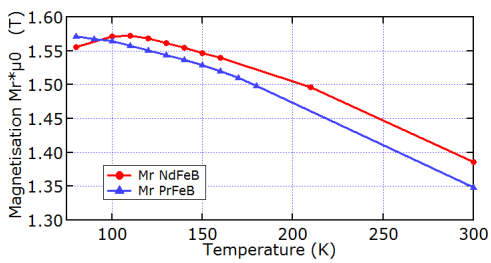

Figure 1: $Nd_2Fe_{14}B$ (red) and $Pr_2Fe_{14}B$ (blue) remanent field dependence with the temperature.

* mathieu.valleau@synchrotron-soleil.fr

ISBN: 978-3-95450-206-6 doi:10.18429/JACoW-FLS2018-THP2WD01

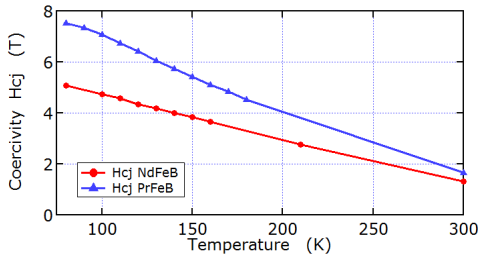

Figure 2: $Nd_2Fe_{14}B$ (red) and $Pr_2Fe_{14}B$ (blue) coercivity dependence with the temperature.

The SOLEIL U18 and U15 undulators characteristics are presented in Table 1. Both undulators have a hybrid structure consisting of $Pr_2Fe_{14}B$ magnets and Vanadium Permendur poles. U18 is 2 m long undulator, that can operate from 5.5 mm to 30 mm gap and provide a peak magnetic field of 1.155 T at cryogenic temperature. U15 is a 3 m long undulator that can operate from 3 mm to 30 mm gap and provide a peak magnetic field of 1.73 T at cryogenic temperature.

Table 1: Main Characteristics of U18 and U15 Undulators

Item	Unit	U18	U15
Technology		Hybrid	Hybrid
Magnet material		CR53	CR53
Remanence	T	1.32 to 1.35 @ 300 K	1.325 @ 300 K
		1.57 @ 77 K	1.55 @ 77 K
Coercivity	kA/m	1835 @ 300 K	1912 @ 300 K
Magnet size (x, z, s)	mm^3	$50 \times 30 \times 6.5$	$50 \times 30 \times 5.5$
Pole material		Vanadium Permendur	Vanadium Permendur
Pole size (x, z, s)	mm^3	$33 \times 22 \times 2.5$	
		$33 \times 22 \times 1.25$	$33 \times 22 \times 1$
Period	mm	18 @ 77 K	15 @ 77 K
Gap range	mm	5.5 to 30	3 to 30
Length	m	2	3
Peak field	T	1.155	1.735

MECHANICAL DESIGN

Figure 3 presents the mechanical design of the cryogenic undulators U18 and U15 inspired from SOLEIL's standard in-vacuum undulators. The carriage is consisting of a metallic base where the frame is welded. Two out-vacuum girders are fixed on the frame and can move vertically thanks to two series of sliders and ball screws. Magnet holders are fixed on two in-vacuum girders connected to the external ones by 36 rods for U15, whereas 24 are needed for U18. The in-vacuum girders are separated by an air gap varying from 3 mm for U15 and 5.5 mm for U18 to 30 mm thanks to two stepper motors. A third one is used to move vertically the undulator over a 10 mm range in order to align in the vertical direction the magnetic axis with the electron beam axis. The vacuum chamber is composed of several ion pumps, titanium sublimation pumps and different instrumentations to ensure an ultra-high vacuum in the vacuum chamber during the operation with electron beam. A 100 μm Cu-Ni foil is placed on the magnetic system and stretched at its extremities of the undulator by a spring-based tensioner system. Permanent magnets are equipped with temperature sensors (PT100) in order to measure the temperature during the cooling down and storage ring operation. Praseodymium based cryogenic undulators are cooled down directly to 77 K, in which the liquid nitrogen crosses the in-vacuum girders through a 12 mm diameter hole, where its inner surface is cooled directly by liquid nitrogen, guaranteeing a better temperature distribution and thus a smaller thermal gradient along the magnetic system.

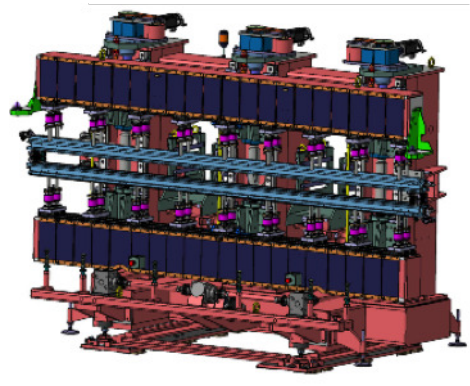

Figure 3: Mechanical design of the U15 cryogenic undulator.

ASSEMBLY OF THE UNDULATOR AT ROOM TEMPERATURE

The assembly and the magnetic corrections of the cryogenic undulators are performed at room temperature in the same conditions as a standard In-Vacuum Undulator (IVU). The figures of merit during the assembly and corrections are the field integrals, trajectories straightness and phase error. They have to be minimized to reduce the impact of the magnetic errors on the undulator performances in terms of photon spectrum and electron beam dynamics.

Modules Assembly and Measurements

As for previous IVUs of SOLEIL, a period of U18 n^{o}1 was constituted by two types of magnet holders. A first one with a single magnet and a second one with a magnet surrounded by two poles. To perform easier swapping after undulator assembly and to allow for a higher number of combinations during assembly, a single module has been designed, which enables to hold a magnet surrounded by two half poles. Figure 4 shows the evolution of modules holder since U18 $_{\text{n}}{}^{o}$1.

Before holders assembly, all the magnets and holders dimensions have been measured and couples have been calculated to reduce the dispersion of magnet altitudes after their mounting on the holders. Then, the poles are assembled on the holders and shimmed to be at the same altitude as the magnet. A specific torque was defined for all the screws so that all the modules are mechanically identical. Then all the modules are characterized using a rotating coil for field integral measurements and a Hall probe to measure the magnetic field profiles.

ISBN: 978-3-95450-206-6 doi:10.18429/JACoW-FLS2018-THP2WD01

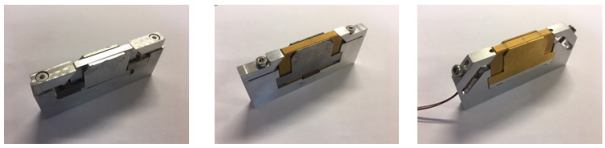

Figure 4: Modules design evolution from U18 n^{o}1 (left), U18 n^{o}2 (middle) and U18 n^{o}3 (right).

Undulator Assembly and Magnetic Corrections

Periods are assembled one by one, two modules on the bottom girder and two on the top one. Each module is adjusted in the longitudinal direction within 15 μm from its theoretical position. For U18 n^{o}2 and 3, all the modules on the girders were vertically pre-shimmed as a function of the magnet altitude and their longitudinal position on the girder. Besides, the longitudinal profile of these girders has been characterized using a Faro laser tracker, ensuring that all the elements of one girder are all at the same altitude. Then, the period is measured using the rotating coil with all the previous periods assembled. A genetic based algorithm software called IDBuilder [16] then deduces the next four convenient modules that fit our requirements.

For U18 n^{o}2 and 3, to obtain optimized trajectories straightness, tighter tolerances have been used during assembly to limit the on-axis field variations from one period to the next one. The on-axis field integrals in both planes should be less than 0.2 G.m, with low variations between two consecutive periods. Also a strong weight is applied so that modules peak field differences should be small.

After the whole assembly of the undulator, the taper of the undulator is adjusted to decrease the phase error and few iterations of rod adjustments are made to correct the low frequency variations of the vertical magnetic field. For all IVUs before U18 n^{o}2, in order to minimize the phase error and optimize the straightness of trajectories, a period of shimming was dedicated to adjust holders or magnets or poles. Thanks to these new mechanical adjustments of magnets and poles on girders and a better control of parameters during assembly, this shimming period was not necessary on U18 n^{o}2 and 3 to reach a very low 2.3 ^{o} and 2.5 ^{o} respectively with an optimized straightness in both planes.

To reduce the effect of the insertion device on the electron beam dynamics, on axis-field integrals have to be minimized so as multipolar terms. After the magic finger correction process on U18 n^{o}3, the on-axis field integrals are less than 0.15 G.m in both planes, integrated gradients are less than 30 G and the off-axis horizontal field integral is reduced from 1.5 G.m to 0.5 G.m and the off-axis vertical field integral from 0.75 G.m to 0.4 G.m.

MEASUREMENTS AND OPTIMIZATIONS AT CRYOGENIC TEMPERATURE

At SOLEIL, magnetic measurements benches have been developed to increase precision and be able to conduct measurements for insertion devices at low temperature. The local magnetic field created by the undulator is measured by a Hall probe (model Bel GH701) and field integrals by a stretched wire. These cryogenic magnetic measurement benches are installed inside the vacuum chamber and removed after the measurements and optimization of the undulator at cryogenic temperature. The Hall probe is mounted on a carriage driven by a stepper motor and slides along a thermalized rail. The position of the Hall probe is measured thanks to a Renishaw interferometer which also triggers the voltmeters. The angular and vertical deformations of the bench are corrected mechanically using shims with different thickness at specific locations. Residual deformations, measured thanks to a laser tracker are then used to correct directly the measured magnetic field.

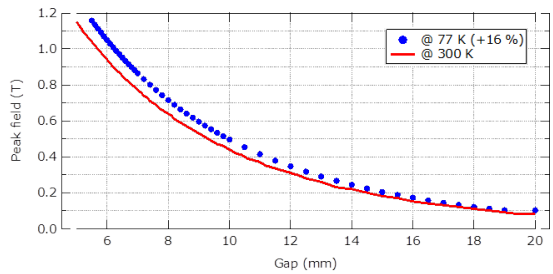

Figure 5: Peak field variation versus gap of U18 n^{o}3 at room (red) and cryogenic temperature (blue).

A temperature variation occurs during the Hall probe displacement along the undulator. The Hall probe resistance and offset dependence with temperature have been calibrated and taken into account to correct the magnetic field values. As shown in Figure 5, at minimal gap, the peak field value is increased by 16 % as expected from the RADIA model [17]. At room temperature, the RMS phase error of U18 n^{o}3 was reduced at 2.45 ^{o} but after cooling down, it increased to 9.5 ^{o}. The rods are contracted vertically by 1.3 mm and in-vacuum girders are contracted longitudinally by 12 mm. These contractions cause in-vacuum girders deformation and the phase error degradation. After few rod adjustments by 5 to 10 μm, the phase error dropped down to 2.6 ^{o} RMS. Figure 6 shows a few variations in the horizontal trajectory straightness and second integral value between room and cryogenic measurements of U18 n^{o}1.

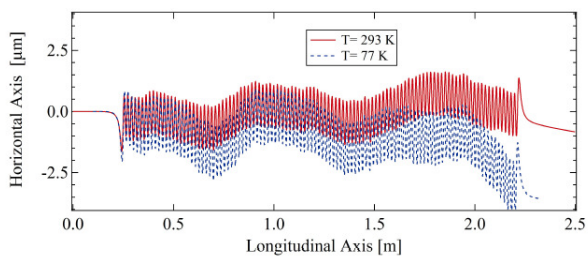

Figure 6: Horizontal trajectory of U18 n^{o}1 at room (red) and cryogenic temperature (blue).

ISBN: 978-3-95450-206-6 doi:10.18429/JACoW-FLS2018-THP2WD01

An evolution of the Hall probe cryogenic bench of U18 is under development for U15 undulator. The major improvement is a dynamic feedback of the Hall probe vertical and horizontal position while moving along the 4 m of the bench [18]. Thanks to Position Sensitive Detectors (PSD), horizontal and vertical positions of the carriage will always be adjusted on the magnetic axis of the undulator thanks to piezo stages, whatever the deformation of the rail guiding the Hall probe. Measurements shows that the thickness and diameter of the pinholes on the hall probe carriage have no effect and that PSD give consistent results thanks to the interferometer (less than 5 μm in both planes).

INSTALLATION ON SOLEIL STORAGE RING

Figure 7 presents the cryogenic undulators U18 n^{o}3 and U18 n^{o}1, installed in the long straight section SDL13 in SOLEIL storage ring. This straight section has been modified to allow for the installation of two canted cryogenic undulators [19] in order to extract two different long beamlines (U18 n^{o}3, dedicated to Anatomix beamline [20] and U18 n^{o}1, dedicated to Nanoscopium beamline) [21].

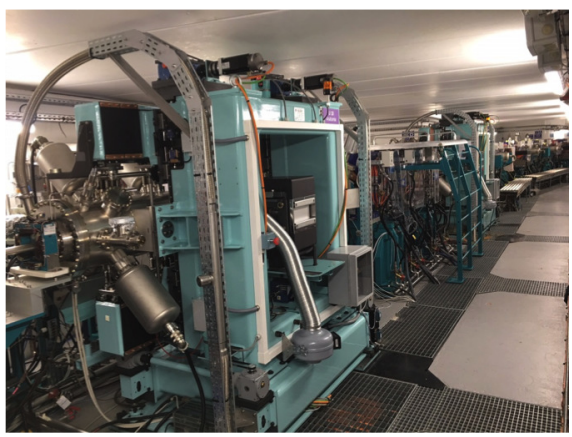

Figure 7: U18 n^{o}3 and U18 n^{o}1 installed in the long straight section 13 of the SOLEIL synchrotron.

Effects on the Electron Beam

After installation and alignment in the tunnel, the magnetic axis has to match with the electron beam path in the straight section. This optimization can be performed at closed gap by moving vertically the entire carriage and observing the vertical betatron tune variations (directly related to the peak magnetic field as shown in Figure 8), or the electron beam decay. Measurements of U18 n^{o}3, shows that this undulator has very low effect on the emittance, injection efficiency and chromaticities between an opened and closed gap.

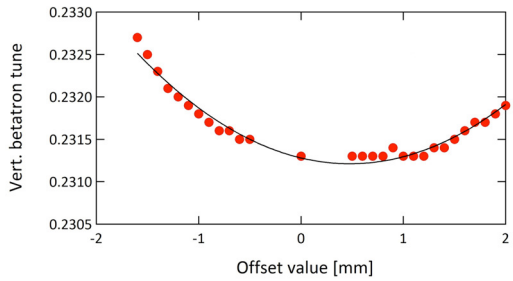

Figure 8: Vertical betatron tune shift variations of the electron beam of U18 n^{o}1 versus the offset of the undulator.

Photon Beam Measurements

The spectrum emitted by the cryogenic undulator U18 n^{o}1 has been measured on the Nanoscopium long beamline [1]. For the beamline commissionning and for regular verifications of the undulator alignment can be performed in a more precise manner in looking at the undulator harmonic shapes for different electron translations or bumps. The vertical offset of the undulator has been adjusted with the beamline so that the electron beam path perfectly matches with the magnetic axis of the undulator. The adjustment has been performed by monitoring the 11 th harmonic for different values of carriage offset, while keeping a magnetic gap of 5.5 mm. Then extracting the intensity and bandwidth of the harmonic, one can find the optimized offset where the intensity is maximal and bandwidth minimal. Same procedure can be applied for taper optimization, by changing the parallelism between top and bottom girders which varies the deflection parameter along the undulator axis. At high energies, few μm of taper can easily be seen. Figure 9 shows the harmonics 9 to 14 of U18 n^{o}1 after offset and taper optimization. It appears that spectra measured on the beamline 77 m away from the source in a 0.1 mm $\times$ 0.1 mm aperture are very close to the ones on an ideal undulator calculated using SRW [22].

Operation with Cryogenic Undulator

At SOLEIL, cryogenic undulators are cooled down with cryo-cooler from Research Instruments. During the 7 years of operation with U18 n^{o}1, only one failure of the cryo-cooler impacted the beam for a few hours. One warming up of the undulator is performed a year due to SOLEIL electrical shutdown. The warming up lasts approximately 24 hours by injecting warm nitrogen gas under 2.5 bar in the undulator. The cooling down of the undulator lasts approximately 6 hours to reach 77 K. The undulator vacuum pressure drops quite rapidly due to the cold mass which acts as a cryo-pump.

ISBN: 978-3-95450-206-6 doi:10.18429/JACoW-FLS2018-THP2WD01

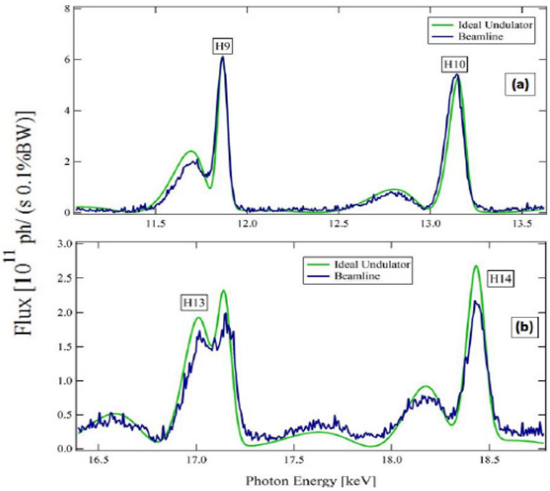

Figure 9: Comparison of the spectra of U18 n^{o}1 measured by Nanoscopium beamline (blue) and the one of an ideal undulator (green).

CONCLUSION

Three cryogenic undulators have successfully been built at SOLEIL, each with a phase error below 3 ^{o} RMS at cryogenic temperatures. New methods of optimizations based on a single module design enables to obtain an optimized undulator directly after assembly (case of the two last cryogenic undulators). These methods will be applied for the assembly of the 3 m long U15 undulator, which will use a SAFALI type bench for measurements at cryogenic temperatures.

ACKNOWLEDGEMENT

The authors thank the SOLEIL-Swedish collaboration for the construction of the U15 undulator. The construction of the ANATOMIX beamline is largely funded by the French National Research Agency (ANR) through the EQUIPEX investment program, project *NanoimagesX*, grant no. ANR-11-EQPX-0031.

REFERENCES

[1] C. Benabderrahmane, M. Valléau, M. E. Couprie *et al*, Development and Operation of a $Pr_2Fe_{14}B$ Based Cryogenic Permanent Magnet Undulator for a High Spatial Resolution X-ray Beamline, Physical Review Accelerators and Beams 20, 033201, (2017)

[2] C. Benabderrahmane, M. Valléau, M. E. Couprie et al, $Nd_2Fe_{14}B$ and $Pr_2Fe_{14}B$ magnets characterization and modeling for cryogenic permanent magnet undulator applications, *Nuclear Instruments and Methods*, A669, pp 1-6, (2012)

[3] T. Hara, T. Tanaka, H. Kitamura, T. Bizen, X. Marechal,T. Seike, T. Kohda, and Y. Matsuura, Cryogenic permanent magnet undulators, *Physical Review Special Topics-Accelerators and Beams*, vol. 7, no. 5, p. 050702, (2004)

[4] T. Tanabe, J. Ablett, L. Berman, D. A. Harder, S. Hulbert, M. Lehecka, G. Rakowsky, J. Skaritka, A. Deyhim, E. Johnson, et al., X-25 cryo-ready in-vacuum undulator at the NSLS, in Synchrotron Radiation Instrumentation; Part One(AIP Conference Proceedings Volume 14879), vol. 879, pp. 283-286, (2007)

[5] T. Tanabe, O. Chubar, D. A. Harder, M. Lehecka, J. Rank, G. Rakowsky, C. Spataro, R. Garrett, I. Gentle, K. Nugent, et al., Cryogenic field measurement of $Pr_2Fe_{14}B$ undulator and performance enhancement options at the NSLS-II, in *Proc AIP Conference*, vol. 1234, p. 29, (2010)

[6] C. Kitegi, P. Cappadoro, O. Chubar, T. Corwin, D. Harder, P. He, H. Fernendez, G. Rakowsky, C. Rhein, J. Rank, et al., Development of a $Pr_2Fe_{14}B$ cryogenic undulator at NSLS-II, Proceedings of International Particle Accelerator Conference, vol. 12, p. 762, (2012)

[7] J. Bahrdt, H. Backer, M. Dirsatt, W. Frentrup, A. Gaupp, D. Just, D. Pfluckhahn, M. Scheer, B. Schulz, et al., Cryogenic design of a PrFeB-based undulator, in *Proc. International Particle Accelerator Conference*, pp. 3111-3113, (2010)

[8] C. Benabderrahmane, P. Berteaud, M. Valléau, C. Kitegi, K. Tavakoli, N. Béchu, A. Mary, J. Filhol, and M. Couprie, $Nd_2Fe_{14}B$ and $Pr_2Fe_{14}B$ magnets characterization and modeling for cryogenic permanent magnet undulator applications, *Nuclear Instruments and Methodsin Physics Research SectionA: Accelerators, Spectrometers, Detectors and Associated Equipment*, vol. 669, pp. 1-6, (2012)

[9] M. Couprie, C. Benabderrahmane, P. Berteaud, F. Briquez, C. Bourassin-Bouchet, F. Bouvet, L. Cassinari, L. Chapuis, M. Diop, J. Daillant *et al*., The status of the LUNEX5 project, Proceedings of Free Electron Laser Conference, vol. 14, (2014)

[10] C. Kitegi, J. Chavanne, D. Cognie, P. Elleaume, F. Revol, C. Penel, B. Plan, and M. Rossat, Development of a cryogenic permanent magnet in-vacuum undulator at the ESRF, vol. 6, pp. 3559-3561, (2006)

[11] C. Ostenfeld and M. Pedersen, Cryogenic in-vacuum undulator at DANFYSIK, Proceedings of International Particle Accelerator Conference, vol. 10, pp. 3093-3095, (2010)

[12] T. Tanaka, T. Seike, A. Kagamihata, H. Kitamura, T. Schmidt, A. Anghel, M. Brugger, W. Bulgheroni, and B. Jakob, In-situ magnetic correction for cryogenic undulators, Proceedings of International Particle Accelerator Conference, vol. 10, pp. 3147-3149, (2010)

[13] M.-E. Couprie *et al*., An application of laser plasma acceleration: towards a free electron laser amplification, Plasma Physics And Controlled Fusion, vol 58, n^{o}3, (2016)

[14] A. Loulergue, M. Labat, C. Evain, C. Benabderrahmane, V. Malka, and M. Couprie, Beam manipulation for compact laser wakefield accelerator based free-electron lasers, *New Journal of Physics*, vol. 17, n^{o}2, 023028, (2015).

[15] D. Givord, H.S. Li., Magnetic properties of $Y_2Fe_{14}B$ and $Nd_2Fe_{14}B$ single crystals, Solid state communications, 51(11), pp 857-860, (1984)

[16] O. Chubar, O. Rudenko and al, Application of genetic algorithms to sorting, swapping and shimming of the SOLEIL undulator magnets, *AIP Conf. Proc.*, 879, 359, (2007)

[17] O. Chubar, P. Elleaume, and J. Chavanne., A three-dimensional magnetostatics computer code for insertion devices, *Journal of synchrotron radiation* 5.3, pp 481-484, (1998)

ISBN: 978-3-95450-206-6 doi:10.18429/JACoW-FLS2018-THP2WD01

[18] T. Tanaka, T. Seike, H. Kitamura, Measurement of SPring-8 XFEL undulator prototype with the SAFALI system, Proceedings of Free Electron Laser Conference, Gyeongju, Korea, pp 371-373, (2008)

[19] A. Somogyi, C. Kewish, F. Polack, and T. Moreno, The scanning nanoprobe beamline NANOSCOPIUM at synchrotron SOLEIL, in *Proc. 10th International Conference on X-ray Microscopy,* vol. 1365, pp. 57-60, (2011).

[20] A. Loulergue, C. Benabderrahmane, F. Bouvet, P. Brunelle, M.-E. Couprie, J.-C. Denad, T. Moreno, A. Nadji, L. Nadolski, F. Polack *et al*, Double low beta straight section for dual canted undulators at SOLEIL, *Proceedings of the IPAC conference*, WEPEA011, pp 2496-2499, (2010).

[21] T. Weitkamp, M. Scheel, J.-L. Giorgetta, V. Joyet, V. Le Roux, G. Cauchon, T. Moreno, F. Polack, A. Thompson, and J.-P. Samama, The tomography beamline ANATOMIX at Synchrotron SOLEIL, *J. Phys. Conf. Series* 849 (2017) 012037, doi:10.1088/1742-6596/849/1/012037

[22] O. Chubar, and P. Elleaume, Accurate and efficient computation of synchrotron radiation in the near field region, in *Proc. EPAC1998.*